Hydrogen Bonding in Water Clusters and Their Ionized Counterparts

ARTICLE *in* THE JOURNAL OF PHYSICAL CHEMISTRY B · DECEMBER 2010

Impact Factor: 3.3 · DOI: 10.1021/jp108634z · Source: PubMed

3 AUTHORS, INCLUDING:

Subha Alladi
Indian Institute of Chemical Technology
14 PUBLICATIONS **319** CITATIONS
SEE PROFILE

G Narahari Sastry
Indian Institute of Chemical Technology
262 PUBLICATIONS **5,292** CITATIONS
SEE PROFILE

Hydrogen Bonding in Water Clusters and Their Ionized Counterparts

Y. Indra Neela, A. Subha Mahadevi, and G. Narahari Sastry*

Molecular Modeling Group, Organic Chemical Sciences, Indian Institute of Chemical Technology, Tarnaka, Hyderabad 500 607, AP, India

Received: September 10, 2010; Revised Manuscript Received: October 29, 2010

Ab initio and DFT computations were carried out on four distinct hydrogen-bonded arrangements of water clusters $(H_2O)_n$, $n = 2-20$, represented as W1D, W2D, W2DH, and W3D. The variation in the strength of hydrogen bond as a function of the chain length is studied. In all the four cases, there is a substantial cooperative interaction, albeit in different degrees. The effect of basis set superposition error (BSSE) on the complexation energy of water clusters has been analyzed. Atoms in molecules (AIM) analysis performed to evaluate the nature of the hydrogen bonding shows a high correlation between hydrogen bond strength and the trends in complexation energy. Solvated water clusters exhibit lower complexation energies compared to corresponding gas-phase geometries on PCM (polarized continuum model) optimization. The feasibility of stripping an electron or addition of an electron increases dramatically as the cluster size increases. Although W3D caged structures are stable for neutral clusters, the helical W2DH arrangement appeared to be an optimal choice for its ionized counterparts.

Introduction

The formation of matter from molecules is governed by the way in which noncovalent interactions operate inter alia. Hydrogen bonding is arguably the most extensively studied among all the noncovalent interactions. The stability of water clusters, based on the arrangement of individual molecules in different phases has been widely explored.[1,2] Numerous theoretical studies have focused on understanding hydrogen bonding in small water clusters $(H_2O)_n$ ($n = 2-6$).[1−11] In one of the carefully conducted computational studies, it was shown that the most stable geometries of water clusters $(H_2O)_n$ ($n = 8-20$) arise from a fusion of tetrameric or pentameric rings.[12] The structure and stability of linear (helical) water chains which are predominant motifs in different host environments as well as spirocyclic water clusters have also been analyzed.[13] Computations performed on dimer, cyclic trimer, and tetramer water clusters show that counterpoise (CP)-corrected interaction energies afford more accurate results than the uncorrected methods.[5]

Correlation of relationship between hydrogen-bonded topology and the energy of water clusters ($n = 8$, 10, 12) indicates that the energy of water cluster depends to a large extent on the placement of non-hydrogen-bonded H-atoms.[14] Extensive studies on the structure and behavior of large water clusters ($n \geq 10$) are also reported.[12−18] The calculated structure of a clathrate like H_2O-buckminsterfullerene (a C_{60} analogue) represents a true minimum structure, where the large volume and an entropic penalty of water cage is compensated by favorable binding energies caused by cooperative effects.[17] Encapsulation of $(H_2O)_n$ clusters ($n = 1-22$) in fullerene cages using gradient-corrected DFT show equilibrium configurations similar to gas phase for small clusters ($n < 12$) while the larger clusters tend to adopt cagelike configurations.[18] Geometrical structures and energetics of likely candidates for global potential energy minima of $C_{60}(H_2O)_n$ clusters up to $n = 21$ were characterized using a theoretically guided empirical potential energy surface and basin-hopping global optimization to reveal a rather hydrophobic water−fullerene interaction.[19]

A wide range of water cluster arrangements in biological systems as well as in other supramolecular aggregations have also been studied.[20−23] They serve the crucial function of lending stability to supramolecular assemblies. Some of the important forms of naturally occurring arrangements of water are represented in Scheme 1a−f. Extensive experimental studies focusing on varied arrangements of water molecules in different forms of ice are known in the literature. Scheme 1a shows a representation of ice XI[24] with *Cmc*21 structure and Scheme 1d which indicates ice in its Ih form.[25] Water decamer $(H_2O)_{10}$ with an icelike molecular arrangement (Scheme 1c) was reported in a supramolecular complex of Cu and Co.[26] Recent studies report the presence of infinite 1D helical chains of water molecules in nanoporous channels of organic hexahosts trichlorophloroglucinol and tribromophloroglucinol (Scheme 1b).[27] Modeling biological water is important to understand solvation of biomolecules such as proteins. Free water species at globular protein surface which are particularly relevant for function are represented in Scheme 1e.[28] Scheme 1f depicts water modeled at micellar surface mimicking biological water at the protein surface.[29] Thus, the constrained microenvironment of organic and metal organic host lattices gives way to multitudes of hydrogen-bonded water cluster arrangements. Thus, it is evident that quite exotic structures which are not minima in the gas phase have a high probability to occur in supramolecular architecture and there is a need to look at the structures which are not minima on potential energy surface.

Besides neutral water clusters, their ionic forms have also been the subject of detailed investigation.[30−33] In a recent study, the relative preference for a 3D structure or a netlike structure for protonated water decamer $H^+(H_2O)_{10}$ is explored using DFT, MP2, CCSD, and CCSD(T) methods.[30] An exhaustive study was performed on a series of multicoefficient correlation methods to test their ability to reproduce neutralization energies for a data set of small hydronium and hydroxide clusters.[31] Theoretical

* To whom correspondence should be addressed. E-mail: gnsastry@gmail.com.

10.1021/jp108634z
Published on Web 12/03/2010

SCHEME 1: Representation of Various Real and Model Systems of Water Clusters[a]

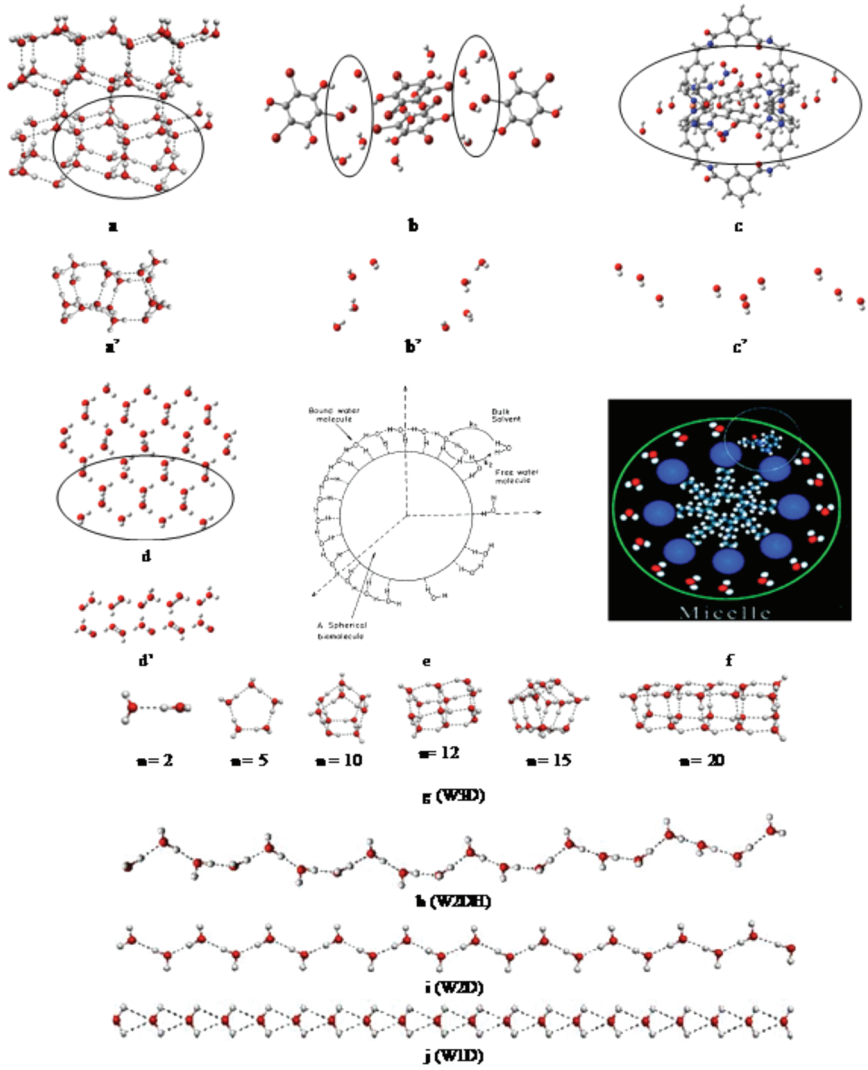

[a] (a) Ice XI, (a′) repeating unit of (a), (b) helical water chain, (b′) repeating unit of (b), (c) supramolecular complex in aqueous media, (c′) repeating unit of (c), (d) ice Ih, (d′) repeating unit of (d), (e) biological water, (f) distribution of water at micellar surface mimicking protein surface.

studies clearly attribute the origin of the magic numbers showing abundance in mass spectra in $e^-(H_2O)_n$ to their positive electron affinity compared to the weak stability of corresponding neutral water clusters for $n = 2$, 6, 7, and 11.[34] The protonated water cluster $[H(H_2O)_n]^+$ ($n = 21$) has also been subject to ab initio calculations to explain its abundance over other clusters and to know whether the proton is strongly bound to a single water molecule (Eigen form; H_3O^+) or if it is shared between two water molecules (Zundel form; $H_2O\cdots H^+\cdots OH_2$).[35a] Simulation studies on $H^+(H_2O)_{21}$ "magic" water cluster reveal how the protonated species in this cluster resides on its surface.[35b] Numerous spectroscopic studies, which consider both ionic and neutral forms of small water clusters as well as bulk liquid, have been reported in the literature.[36−38] Molecular dynamics approaches too have been avidly applied on water clusters of different sizes.[39] Using an all-exchanges parallel tempering Monte Carlo method, the impact of application of a uniform electric field on the behavior of small water clusters $(H_2O)_n$ ($n = 2-5$ and $n = 8$) has been explored both as a function of temperature as well as strength of electric field.[40] A combined approach of a basin-hopping algorithm along with an empirical, polarizable model potential has been employed to get global minima for protonated water clusters.[41]

An important concept associated with hydrogen bonding is cooperativity.[42] Several noncovalent interactions have a mutually enhancing effect over each another. This phenomenon is defined as cooperativity.[43] The cooperative effect of hydrogen bonding in ice has been explored initially with ab initio calculations at HF and MP4 levels on an infinite water chain as a model system.[2] The way in which hydrogen bonding operates is clearly understood by a study on formamide−water complexes where B3LYP method shows better performance over MP2 for studying interactions in hydrogen-bonded complexes.[44] The maximization of the nonadditive component of binding energy leading to cooperativity too has been explored in clusters of water molecules.[6] Quantum mechanical calculations have been proved to be extensively useful to study the effect of solvation on noncovalently bound complexes.[45] Solvation has a profound influence on the binding of metal ion with aromatic systems and can dramatically modulate the strength of complexation depending on the site of solvation.[46]

In the present study, we have undertaken a computational analysis of three linear forms of water cluster arrangements to gauge their relative stability and reactivity. Theoretical calculations have been performed from dimer to eicosamer of water clusters (Scheme 1h−j) using HF, DFT, and MP2 methods. The

caged clusters of $(H_2O)_n$ ($n = 2-20$) (Scheme 1g) obtained from the Cambridge Cluster Database (CCD)[23a,47] have been widely employed in earlier ab initio investigations and here we employ them as a standard reference. The impact of various levels of theory and basis sets employed in the calculations along with the effect of basis set superposition error on complexation energy of the water clusters is explored. Very subtle factors such as the size of the system and change in the nature of bond formation in clusters can substantially modulate the strength of the nonbonded interactions.[48,49] Here we dwell upon the phenomenon of cooperativity in the context of water clusters. The results of AIM analysis followed by PCM analysis are then discussed. Finally, the issue of relative stability of ionized form of all water clusters taken is addressed. The study is expected to give the relative propensity of various water cluster arrangements toward ionization.

Computational Details

The model systems considered for the present study are neutral water clusters ($(H_2O)_n$; $n = 2-20$) denoted as W1D, W2D, W2DH, and W3D wherein four distinct modes of hydrogen bonding are represented (Scheme 1g−j). W1D and W2D represent a linear assembly of water molecules, W2DH represents a helical arrangement ($(H_2O)_n$; $n = 6-20$), and W3D consists of structures obtained from Cambridge Cluster Database. Geometry optimizations were carried out on all the water cluster arrangements at HF, B3LYP, and MP2 levels of theory with 6-311+G* basis set. All the computations were performed using the Gaussian 03 program package.[50] Besides this, in the case of W1D, W2D, and W3D arrangements, optimizations were also done at the HF level with 6-31G* and 6-31G** basis sets, at the B3LYP level with 6-31G*, Dunning's type correlation consistent (cc-pVDZ and aug-cc-pVDZ) basis sets, and at the MP2 level of theory with 6-31G* basis set. However, W2DH clusters were subjected to optimization at HF, B3LYP, and MP2 levels of theory using 6-311+G* basis set alone. The complexation energy (IE) of a cluster is calculated using eq 1 given below.

$$\mathrm{IE} = E_{\mathrm{total}} - nE_{\mathrm{monomer}} \tag{1}$$

where E_{total} is the total energy of water cluster and E_{monomer} is the total energy of a single water molecule.

The complexation energy per hydrogen bond is defined as IE/n − 1 (where n indicates number of monomers in a given cluster ranging from 2 to 20). Optimized geometries of W1D and W2D clusters are constrained to C_{2v} and C_s symmetry and are not minima on potential energy surface. However, W2DH and W3D clusters are minima with C_1 symmetry with the exception of $(H_2O)_n$ (n = 4, 8, 12, 16, and 20) of W3D arrangement having S_4 symmetry. To evaluate the extent of basis set dependence, single-point calculations were done at the B3LYP level using 6-31G*, 6-31G**, 6-311+G*, 6-311++G**, cc-pVDZ, aug-cc-pVDZ, cc-pVTZ, and aug-cc-pVTZ basis sets on B3LYP/6-311+G*-optimized geometries. The complexation energy was then corrected for basis set superposition error (BSSE) using the counterpoise correction (CP) scheme proposed by Boys and Bernardi.[51] The ratios of BSSE-corrected and uncorrected complexation energy per hydrogen bond from dimer to decamer and from decamer to eicosamer are represented as ($[H_2O_{10:2}]$ and $[H_2O_{20:10}]$). Following this, electron density at the bond critical point in all the structures was mapped using the AIM2000 program[52] at the B3LYP/6-311+G* level. The existence of bond critical points corresponding to H-bonding is noted and their quantitative characteristics are studied. Further, PCM[53] optimizations with water as implicit solvent were performed at the B3LYP/6-311+G* level for clusters up to decamer to get an indication of effect of presence of solvent on complexation energy.

The cationic $(H_2O)_n^{\bullet+}$ and anionic $(H_2O)_n^{\bullet-}$ radical counterparts of the four water cluster arrangements were generated. The calculated ionization potential (IP) and electron affinity (EA) of the corresponding optimized ionic radicals refer to the adiabatic ionization potential (IP_A) and adiabatic electron affinity (EA_A). Similarly, the vertical ionization potential (IP_V) corresponds to the energy difference between the cationic radical in the geometry of the neutral state and the optimized neutral state, whereas the vertical electron affinity (EA_V) refers to the energy difference between the optimized neutral state and the anionic radical in the geometry of neutral state. Therefore, a positive EA implies that the anion radical is lower in energy than its corresponding neutral parent molecule and hence stable, whereas a negative value means that the anion radical is unstable with respect to electron detachment. The reorganization energies of respective clusters were evaluated using eq 4. Reorganization energy (RE) is the energy difference between the optimized charged state and the charged state in the geometry of its neutral state, which can be used to evaluate the structural changes for the charged state in the geometry of the neutral state.[54]

$$\mathrm{IP} = E_{\mathrm{cc}} - E_{\mathrm{nc}} \tag{2}$$

$$\mathrm{EA} = E_{\mathrm{nc}} - E_{\mathrm{ac}} \tag{3}$$

where E_{nc} is the total energy of neutral water cluster, E_{cc} the total energy of cationic water cluster, and E_{ac} the total energy of anionic water cluster.

$$\text{reorganization energy (RE)} = E_{\mathrm{A}} - E_{\mathrm{V}} \tag{4}$$

where E_{A} is the total energy of the optimized ion cluster and E_{V} the single-point energy of ion on neutral cluster geometry.

NPA analysis was performed on four arrangements of neutral and ionic water clusters. A method of "natural population analysis" (NPA)[55] has been developed to calculate atomic charges and orbital populations of molecular wave functions in general atomic orbital basis sets. The natural population analysis

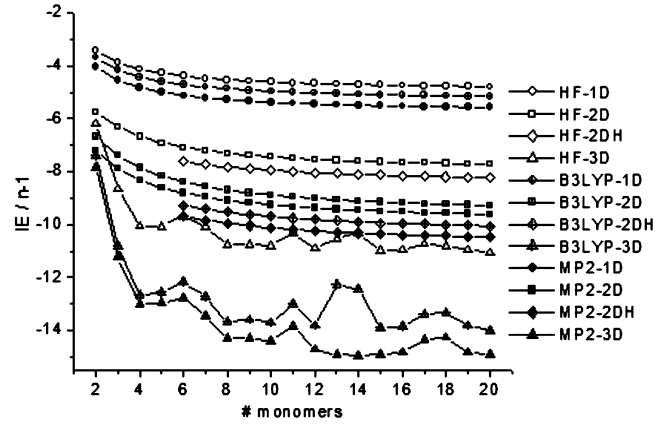

Figure 1. Comparison of interaction energy per hydrogen bond (IE/n − 1 in kcal/mol) for W1D, W2D, W2DH, and W3D arrangements at HF, B3LYP, and MP2 level of theory using 6-311+G* basis set.

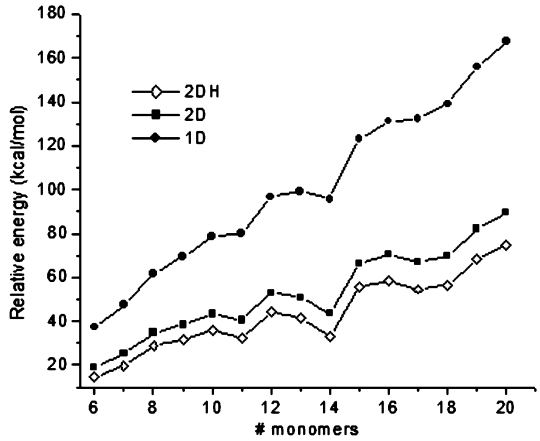

Figure 2. Relative energies of W1D, W2D, and W2DH water cluster arrangements with respect to the total energies of W3D clusters optimized at the B3LYP/6-311+G* level of theory.

is an alternative to conventional Mulliken population analysis, and seems to exhibit improved numerical stability and to better describe the electron distribution in compounds of high ionic character. In this study, we have used NPA to examine the charge transfer between water molecules in their ionic form. Based on these NPA charges, Fukui function indices[56] were calculated for the model systems and their counterions. The Fukui function, $f(r)$, is defined as the change of the electron density $\rho(r)$ at each point r corresponding to change in the total number of electrons. Yang and Mortier have proposed an approach to calculate the Fukui function index at an atom k based on electronic population by applying finite difference approximation.

$$f_k^+ = q_k(N_0 + 1) - q_k(N_0) \quad \text{(for nucleophilic attack)} \tag{5}$$

$$f_k^- = q_k(N_0) - q_k(N_0 - 1) \quad \text{(for electrophilic attack)} \tag{6}$$

$$f_k^\bullet = qk(N_0 + 1) - qk(N_0 - 1) \quad \text{(for radical attack)} \tag{7}$$

where $q_k(N_0)$, $q_k(N_0 - 1)$, and $q_k(N_0 + 1)$ denote the electronic population on atom k for N_0, $N_0 - 1$, and $N_0 + 1$ electronic systems, respectively.

Results and Discussion

Effect of Method on Complexation Energy. The variation in complexation energy per hydrogen bond with increase in size of water cluster from dimer to eicosamer ($(H_2O)_n$; $n = 2-20$) at HF, B3LYP, and MP2 levels of theory using 6-311+G* basis set is shown in Figure 1. In all the four modes of arrangements (W1D, W2D, W2DH, and W3D), the maximum complexation energy is observed for water clusters optimized at MP2 level of theory followed by B3LYP and HF levels of theory.

The complexation energy of water clusters follows the order W3D > W2DH > W2D > W1D. A steeper increase in complexation energy is noted from dimer to decamer than from decamer to eicosamer for W1D, W2D, and W2DH clusters. In the case of W1D arrangement, a complexation energy difference of ~0.4−0.6 kcal/mol is observed between HF-B3LYP and B3LYP-MP2 levels. In the case of W2D, W2DH, and W3D arrangements, a complexation energy change of ~0.9−1.5 kcal/mol is seen in between HF-B3LYP levels and a difference of ~0.5 kcal/mol is seen in between B3LYP-MP2 levels. This difference in complexation energy is observed in all clusters as we move from dimer to eicosamer. The relative energy (kcal/mol) of W1D, W2D, and W2DH clusters in comparison to the highly stable caged W3D structures at B3LYP/6-311+G* are plotted in Figure 2.

A cursory look at this figure shows that W2D and W2DH arrangements have ~15−85 kcal/mol higher energy compared to corresponding W3D clusters as the cluster size increases from hexamer to eicosamer. The W1D arrangement has relative energy severalfold higher than the reference W3D arrangement-.The complexation energy per hydrogen bond for all the clusters optimized at different levels of theory using various basis sets are presented in Table S1 in the Supporting Information.

Effect of Method on Optimized Geometries. A representative example of water dimer ($n = 2$) is taken to demonstrate the impact of three (HF, B3LYP, MP2) methods on the hydrogen bond distance observed in the optimized geometries (Table 1).

The value of hydrogen bond distance present in the dimer is computed and on its basis a comparison of the four arrangements is made. The results in Table 1 indicate the following trend for O−H bond distance in dimer: W1D > W3*D* = W2DH > W2D. In all the four arrangements, the O−H bond distance at HF level is higher than at the B3LYP and MP2 levels of theory. The O−H bond distance at MP2 level is higher by 0.014−0.033 Å than the corresponding distance at B3LYP level. An important observation in the linear chain arrangement of W1D, W2D, and W2DH clusters is the shorter hydrogen bond distance toward the central portion of the chain compared to the terminal hydrogen bonds (Figure 3). The overall average hydrogen bond distance for all the four arrangements at HF, B3LYP, and MP2 levels is higher for clusters $n = 2-10$ than for clusters from $n = 10 - 20$.

While W1D and W2D clusters have 0.030−0.038 Å higher average O−H bond distance for $n = 2-10$ compared to $n = 10-20$, a difference of 0.016−0.038 Å is seen for W2DH and W3D clusters. All the water cluster arrangements show average O−H bond distances which are in the range of typical O−H···O hydrogen bond distances.[57] The geometries of all the W1D, W2D, W2DH, and W3D cluster arrangements ($(H_2O)_n$; $n = 2-20$) optimized at HF, B3LYP, and MP2 levels of theory using 6-311+G* basis set are provided in the Supporting Information (Table S3a−d and Figures S1−S4).

TABLE 1: Average O−H Bond Distance (in Å) of W1D, W2D, W2DH (6−10), and W3D Cluster Arrangements ($(H_2O)_n$; n = 2, 2−10, 10−20) at HF, B3LYP, and MP2 Levels of Theory Using 6-311+G* Basis Set (n = No. of Monomers)

	W1D			W2D			W2DH			W3D		
n	2	2−10	10−20	2	2−10	10−20	2	6−10	10−20	2	2−10	10−20
HF	2.667	2.562	2.531	2.001	1.909	1.880	2.001	1.880	1.862	1.985	1.955	1.995
B3LYP	2.567	2.466	2.435	1.900	1.790	1.752	1.900	1.753	1.730	1.879	1.813	1.851
MP2	2.600	2.496	2.466	1.914	1.815	1.784	1.914	1.776	1.757	1.897	1.837	1.853

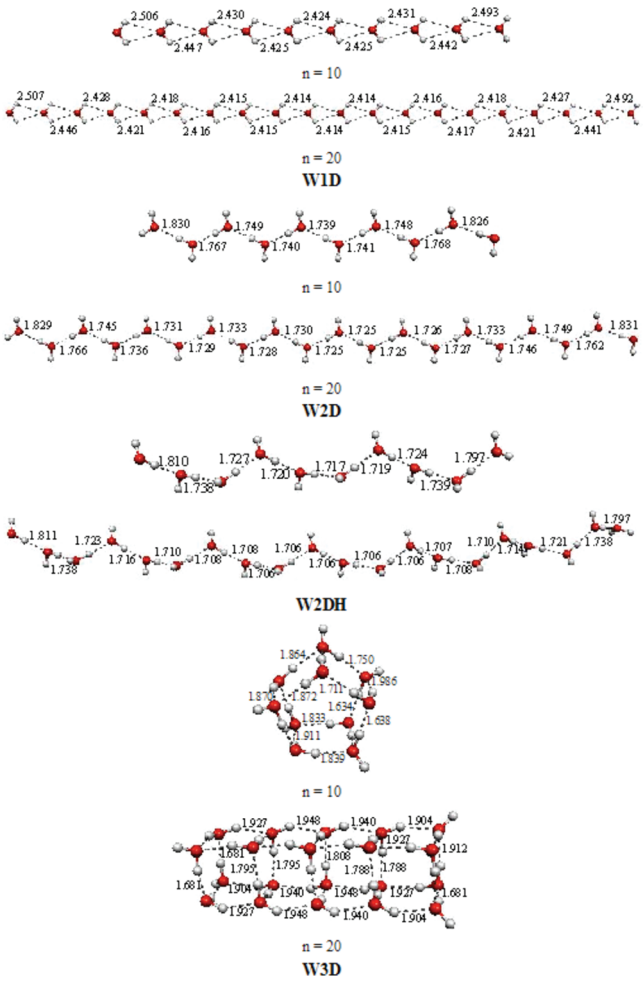

Figure 3. B3LYP/6-311+G*-optimized geometries of W1D, W2D, W2DH, and W3D clusters (n = 10, 20). All bond lengths are given in Å.

Effect of Basis Set on Energy. The impact of different basis sets along with basis set superposition error (BSSE) is shown in Figure 4.

The B3LYP/6-311+G*-optimized geometries were used for single-point calculations with 6-31G*, 6-31G**, 6-311+G*, 6-311++G**, cc-pVDZ, aug-cc-pVDZ, cc-pVTZ, and aug-cc-pVTZ basis sets for all water clusters. The difference between BSSE-corrected and uncorrected complexation energy ratios ([$H_2O_{10:2}$], [$H_2O_{20:10}$]) are about 3−4% for 6-311+G* basis set whereas it is 8−14% in all other cases except with the 6-311++G** basis set. However, there is a minor variation in complexation energy of ∼2% between 6-311+G* and 6-311++G** basis sets.

Cooperativity. The ratio of complexation energy per hydrogen bond from decamer to dimer [$H_2O_{10:2}$] and eicosamer to decamer [$H_2O_{20:10}$] is calculated to quantify the strength of hydrogen bond with increase in cluster size (Table 2) and is used as an indicator of cooperativity that is seen in the water clusters.

Among the basis sets used for single-point calculations, aug-cc-pVTZ shows maximum ratio of complexation energy as the cluster size increases from dimer to decamer in the case of W1D, W2D, and W2DH clusters. In the case of W3D, this ratio is maximum with 6-31G** followed by 6-31G* basis set. The complexation energy ratios ([$H_2O_{10:2}$], [$H_2O_{20:10}$]) of BSSE-corrected single-point calculations with 6-311+G* basis set for W1D (1.33, 1.040), W2D (1.380, 1.050), W2DH (1.352, 1.040), and W3D (1.913, 1.030) show that the strength of complexation energy increases by 33, 38, 35 and 91%, respectively, as cluster size increases from 2 to 10. However, as the cluster size increases from 10 to 20, the increase in strength of hydrogen bonding is in the range of 4−6% only. This is valid in all the calculations where split valence basis sets have been used. A similar trend is observed when correlation-consistent basis sets are used. Thus, the nonadditivity of hydrogen bond strength (cooperativity) is much more evident as cluster size increases from 2 to 10 rather than from 10 to 20, where the augmentation of hydrogen bond strength is only marginal for all the four arrangements.

Electron Density Analysis. It is interesting to note the electron density between two monomers in a complex. For the characterization of hydrogen bonding, the electron density at bond critical points was taken into account. In this context, we have used the atoms in molecules (AIM) approach to note the electron density (ρ) and Laplacian of ρ ($\nabla^2\rho$) at the bond critical point. According to AIM theory, any chemical bond including hydrogen bonding is characterized by the presence of so-called bond critical points (BCP). The bond critical points (3, −1) are characterized by a rank of 3 and a signature of −1. This means that the electron density at this point has a minimal value along the line of the bond and a maximal value in two orthogonal directions. Figure 5 gives a picture of how average electron density (ρ) of a water cluster behaves with increase in cluster size.

The average ρ value increases substantially as cluster size increases from 2 to 10 in comparison to an increase in cluster size from 10 to 20. The magnitude and range of variation of average ρ is maximum in the case of W3D (0.030−0.063 au) compared to W2DH (0.027−0.043 au), W2D (0.027−0.039 au), and W1D arrangements (0.009−0.012 au). There is a high correlation between hydrogen bond strength, estimated on the basis of average of ρ and the trends in complexation energy as cluster size increases from dimer to eicosamer. It is observed that the electron density values at the bond critical point of the hydrogen bonds present toward the center of the linear chain of W1D, W2D, and W2DH arrangements are marginally higher in magnitude when compared to terminal H-bonds. The topological maps of all the AIM calculations performed are available in the Supporting Information.

Solvent Effect. PCM optimization with water as implicit solvent was performed at B3LYP/6-311+G* level of theory to get an indication of effect of presence of solvent on complexation energy of the clusters. Though the complexation energy values in the solvated clusters were lower than corresponding gas-phase geometries, their trends remain the same especially for larger clusters (W3D > W2DH > W2D > W1D) (Table 3).

A 4−5 kcal/mol decrease in complexation energy was noted from gas to solvent phase optimization in the case of W1D, W2D, and W2DH arrangements. W3D, however, shows a greater decrease in complexation energy of 6−8 kcal/mol. The total energy of W1D, W2D, and W2DH clusters along with their relative energy with respect to W3D are shown in Table S7a,b in the Supporting Information. The average O−H bond distances for PCM optimized W1D, W2D, and W2DH clusters are 2.480, 1.756, and 1.739 Å, respectively. In the case of W1D clusters, there is an increase in O−H bond distance in solvent phase compared to its gas phase (2.466 Å) while the inverse is observed for W2D (gas phase −1.790 Å) and W2DH clusters (gas phase −1.753 Å) from dimer to decamer. All the PCM-optimized geometries of W1D, W2D, W2DH, and W3D clusters from dimer to decamer are given in the Supporting Information.

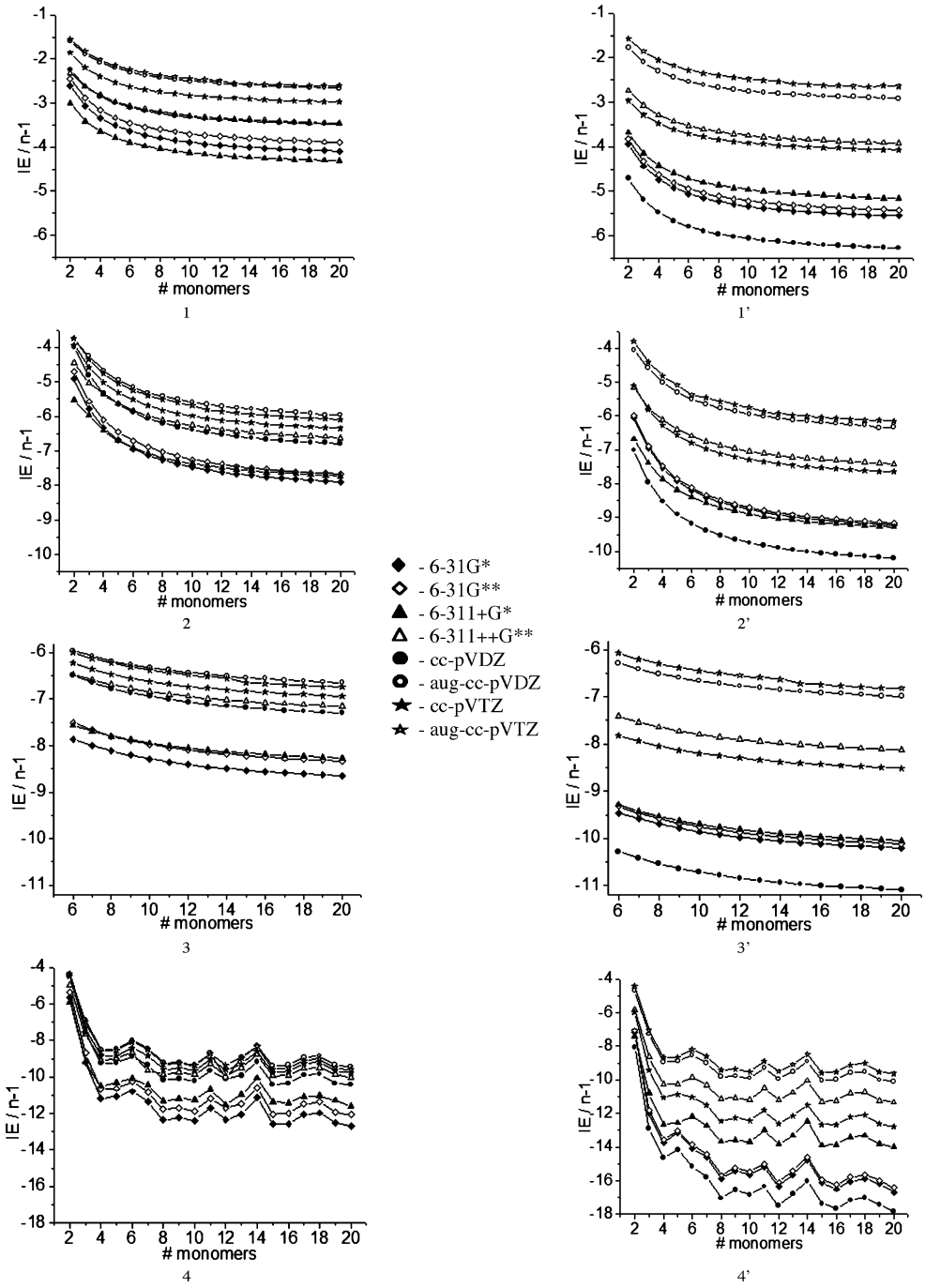

Figure 4. Comparison of counterpoise-corrected (1, 2, 3, 4) and uncorrected (1′, 2′, 3′, 4′) single-point interaction energies (IE/n − 1) of W1D (1, 1′), W2D (2, 2′), W2DH (3, 3′), and W3D (4, 4′) water clusters at B3LYP level of theory using (◆) -6-31G*, (◇) -6-31G**, (▲) -6-311+G*, (△) −6-311++G**, (●) -cc-pVDZ, (○) -aug-cc-pVDZ, (★) -cc-pVTZ, and (☆) -aug-cc-pVTZ basis sets.

TABLE 2: Counterpoise-Corrected Complexation Energy Per Hydrogen Bond of $(H_2O)_{10:2}$ and $(H_2O)_{20:10}$ at B3LYP Level Using Various Basis Sets

		basis sets							
type		6-31G*	6-31G**	6-311+G*	6-311++G**	cc-pVDZ	aug-cc-pVDZ	cc-pVTZ	aug-cc-pVTZ
W1D	a[a]	1.496	1.516	1.370	1.426	1.482	1.572	1.521	1.574
	b[a]	0.997	1.051	1.040	1.050	1.048	1.064	1.053	1.053
W2D	a	1.521	1.539	1.380	1.406	1.601	1.491	1.524	1.518
	b	1.057	1.057	1.050	1.057	1.062	1.066	1.058	1.072
W2DH	a	1.464	1.484	1.352	1.376	1.552	1.435	1.487	1.473
	b	1.043	1.046	1.040	1.046	1.051	1.050	1.048	1.056
W3D	a	2.183	2.208	1.913	1.987	2.285	2.115	2.152	2.166
	b	1.025	1.016	1.030	1.017	1.018	1.011	1.011	1.011

[a] a = IE/n − 1 [$(H_2O)_{10:2}$]. b = IE/n − 1 [$(H_2O)_{20:10}$].

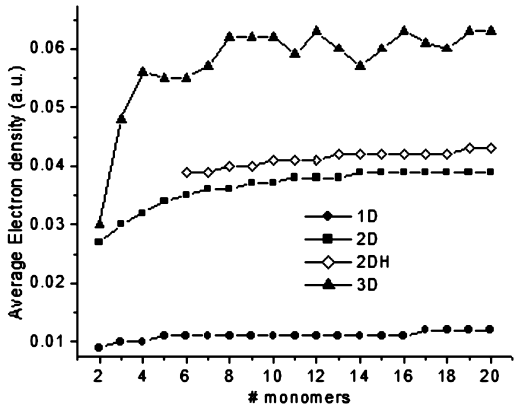

Figure 5. Variation in average electron density with increase in size of water cluster ($n = 2-20$) at the B3LYP/6-311+G* level of theory.

TABLE 3: Comparison of Complexation Energy Per Hydrogen Bond (IE/n − 1 in kcal/mol) for W1D, W2D, W2DH, and W3D Water Cluster Arrangements in the Gas Phase (GP) and Solvent Phase (SP) Optimized at B3LYP/ 6-311+G* level of theory (n = No. of Monomers)

	1D		2D		2DH		3D	
n	GP	SP	GP	SP	GP	SP	GP	SP
2	−3.68	0.27	−6.68	−3.34	*a*	*a*	−7.40	−3.67
3	−4.15	0.26	−7.38	−3.61	*a*	*a*	−10.80	−3.02
4	−4.42	0.25	−7.85	−3.72	*a*	*a*	−12.65	−5.00
5	−4.59	0.27	−8.17	−3.78	*a*	*a*	−12.56	−5.31
6	−4.71	0.27	−8.39	−3.82	−9.28	−4.17	−12.18	−4.40
7	−4.80	0.26	−8.56	−3.86	−9.42	−4.20	−12.73	−5.02
8	−4.86	0.26	−8.70	−3.87	−9.53	−4.22	−13.67	−5.23
9	−4.92	0.27	−8.80	−3.88	−9.62	−4.23	−13.59	−5.50
10	−4.96	0.27	−8.88	−3.89	−9.70	−4.24	−13.70	−5.59

[a] For W2DH the cluster size starts from $n = 6$.

Thus, the greater stability of W3D arrangement may be reinforced on the basis of PCM optimization calculations.

Cation and Anion Radicals of Neutral Water Clusters. The ionized counterparts of water clusters were generated. A comparison of the ionization potential (IP) and electron affinity (EA) values was made on the basis of single-point calculations performed on neutral geometries (vertical) as well as those subject to geometry optimization (adiabatic). All the optimized geometries and energies of cationic and anionic radical clusters are available in the Supporting Information (Figures S13−S20; Tables S10 and 11). IP and EA values obtained in vertical and adiabatic calculations are plotted in Figure 6, indicating the relative preference of each cluster arrangement toward cation and anion radical formation.

In the case of W1D, IP_V (vertical ionization potential) and IP_A (adiabatic ionization potential) values are similar. The same holds true for EA_V (vertical electron affinity) and EA_A (adiabatic electron affinity), signaling absence of any drastic change in geometry even upon optimization of cluster after addition/ removal of electron. The average O−H bond distance in the cationic and anionic radical structures of W1D ($n = 2-20$) are 2.378 and 2.430 Å, respectively, which is lower compared to their neutral arrangement (2.442 Å).

For the W2D arrangement, the decrease in IP_A is steeper from $n = 2-5$ than from $n = 6-20$. The adiabatic IP value from $n = 6-20$ is similar to the vertical IP observed. In the case of comparison of electron affinities between adiabatic and vertical calculations, water $n = 7$, 12−15, and 17−20 show slightly higher adiabatic EA values than the vertical arrangements. The average O−H bond distances in the cationic and anionic radical clusters of W2D are 1.679 and 1.750 Å, respectively. Both the cationic and anionic radical clusters show a change in geometry when compared to the neutral water clusters of same size. W2D cation radicals do not show a drastic change in their geometry as compared to the corresponding anion radicals. In the case of cationic radical clusters from $n = 2-5$, we observe the formation of a hydronium ion in the central portion of the chain. This formation of hydronium ion is not seen from $n = 6-20$; they still retain their linear form. The anionic radical clusters show a change in their geometry from dimer onward: one end of the linear chain changes its conformation to a more cyclic form while the other end retains its linear conformation.

The W2DH ions show a similar trend for IP and EA values in both vertical and adiabatic calculations. However, in the case of IP_V and IP_A a difference of 1.2−1.5 eV is noted for $n = 6-13$ and a slightly higher difference of 1.9−2.4 eV is observed from $n = 14-20$. On the other hand, EA_V and EA_A differ by 0.75−1.2 eV for clusters from $n = 6-13$ and 1.15−1.95 eV for $n = 14-20$. The average O−H bond distance in the cationic and anionic radical clusters of W2DH are 1.690 and 1.790 Å, respectively. The optimized geometries of ionized W2DH clusters are quite different from the corresponding neutral clusters. The optimized W2DH cationic radical clusters retain their helical arrangement from $n = 6-13$, with formation of hydronium ion toward the center of the chain. From $n = 14-20$, one end of the helical chain shows greater rearrangement in geometry with the formation of cage like structures at that end. In comparison to optimized W2DH cationic radical clusters, the anionic radical clusters show greater extent of geometry change. The helical form of the corresponding neutral clusters is altered from $n = 6$ onward itself, where the geometries show bending of the chain on both of its ends. From $n = 10$ onward, akin to their cationic radical counterparts, we observe an alteration in the geometry. At one end of the chain, water molecules aggregate in a cagelike fashion, losing their original helical structure, leaving the other end in helical manner. These clusters thus exhibit a head−tail kind of arrangement.

The IP_A values are lower than IP_V in the case of W3D structures with a difference of 0.15−1.83 eV. W3D anion radicals show a minor difference in EA_A and EA_V. The difference observed here is not uniform like W2DH clusters. The clusters $n = 4$, 8, 12, 16, and 20 retain comparable values of IP for both vertical and adiabatic calculations. The other W3D clusters have slightly lower values of IP for adiabatic calculations up to $n = 16$. The W3D EA_V values are quite similar to EA_A values in the case of W3D cluster anion radicals with a difference of 0.3 eV. The neutral clusters from $n = 8$ onward are stacks of four or five water molecules in each stack. This stacking arrangement of water molecules is still intact in both W3D anion and cation radicals even upon optimization. From $n = 2-7$, there is no gross change in optimized geometries of ion radicals compared to their neutral forms. However, a definitive change in orientation of some water molecules is seen in all the clusters.

The discussion so far emphasized the behavior of ionic radicals of each individual arrangement. The subsequent discussion relates the analysis of comparison of IP_V, IP_A, EA_V, and EA_A with the increase in cluster size from dimer to eicosamer ($(H_2O)_n$; $n = 2-20$) for all the four modes of water cluster arrangements. Among the four water clusters, W3D has the maximum IP_V and EA_V, followed by W2DH, W1D, and W2D clusters. The order of IP_A among the four modes of clusters is W3D > W1D > W2D > W2DH. In the case of W3D, the clusters of 4, 8, 12, and 16 water molecules have high IP_A values

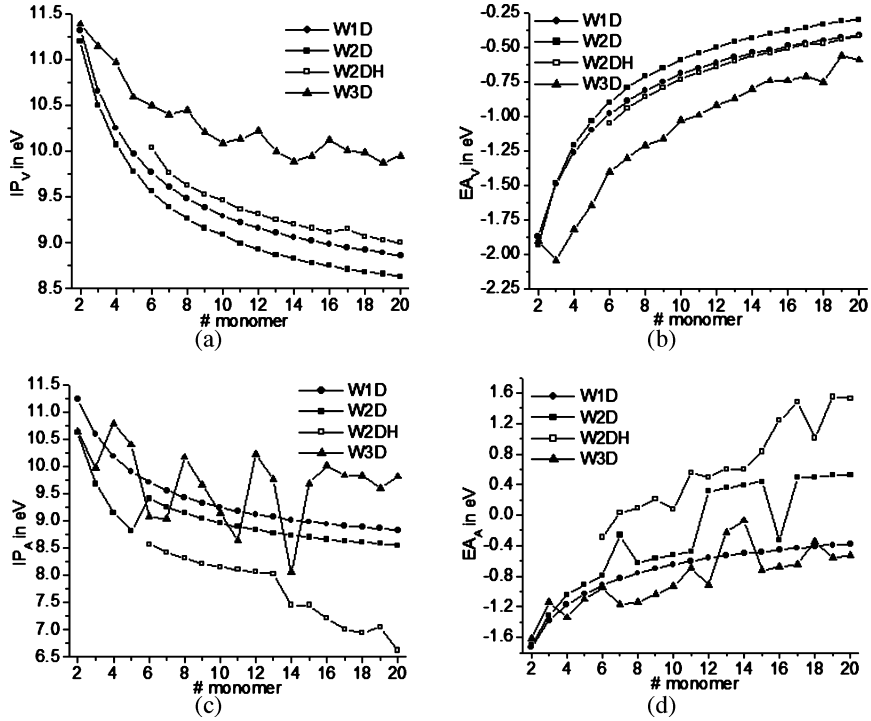

Figure 6. Comparison of (a) vertical ionization potential (IP_V), (b) vertical electron affinity (EA_V), (c) adiabatic ionization potential (IP_A), and (d) adiabatic electron affinity (EA_A) in four arrangements of water clusters at B3LYP/6-311+G* level of theory.

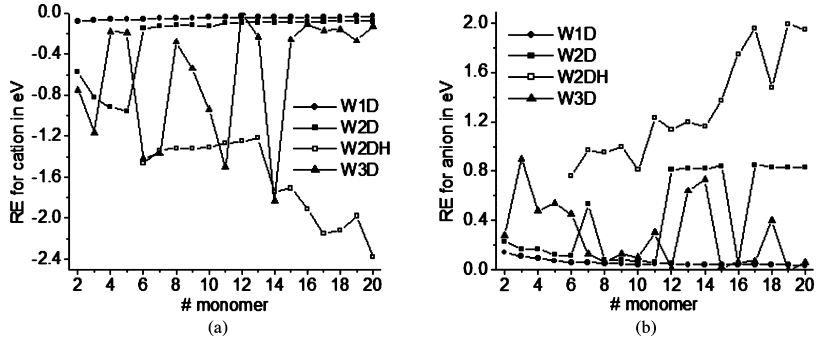

Figure 7. Reorganization energy (kcal/mol) vs size of the cluster for four modes of (a) cationic and (b) anionic water cluster arrangements of B3LYP/6-311+G*-optimized geometries.

compared to all the clusters. This behavior of the clusters is attributed to their geometry which has S_4 symmetry in all the cases. The W2DH have maximum EA_A values compared to all the other arrangements and the least EA_A is shown by W3D clusters. The order of EA_A is W2DH > W2D > W1D > W3D. The water clusters $(H_2O)_n^{\bullet-}$, where $n = 3$, 13, 14, and 18, in W3D arrangement show higher EA_A compared to W1D clusters, others being less than W1D clusters. Thus, the relative propensity of all the arrangements toward ionization reveals highest tendency for ion formation in the case of W2DH clusters.

Figure 7 gives a picture of the reorganization energies of the model systems considered. Reorganization energy of cationic and anionic radical clusters obtained show uniformly low values for W1D model systems as the cluster size increases from $n = 2-20$ when compared to other arrangements. In the case of W2D cationic radicals, the smaller sized clusters up to pentamer show higher reorganization energies (−0.57 to −0.96 eV) compared to the reorganization energies of larger ($n = 6-20$) water clusters (−0.15 to −0.08 eV). In contrast, the W2D anionic radicals have higher reorganization energy in the larger ($n = 12-20$) water clusters (0.81−0.83 eV). W2DH ionic radicals have significantly higher reorganization energies than the other three arrangements irrespective of cluster size, the values ranging between −1.47 and −2.38 eV for cationic radicals and 0.76−1.95 eV for anionic radicals. Reorganization energies observed in the case of W3D arrangement are lesser in strength than W2DH, ranging from −0.75 to −0.13 eV for cationic radicals and 0.28−0.06 eV for anionic radicals from $n = 2-20$. The order of reorganization energy for cationic radical water clusters, $n = 2-20$, among the four modes of arrangement is W2DH > W3D > W2D > W1D and for anionic radical water clusters is W2DH > W2D > W3D > W1D, respectively.

An indication of relative reactivities of the different oxygens in the water cluster ions based on the Fukui function indices calculated can be obtained on perusal of Figure 8.

All the oxygen atoms except the terminal ones in all four water cluster arrangements have nearly same Fukui function indices. Fukui function indices on all oxygen atoms for $(H_2O)_n$ ($n = 20$) cationic radical in four different arrangements for vertical and adiabatic states show maximum value (0.797, 1.246) on terminal oxygen of W2DH water molecule. Corresponding Fukui function indices for $(H_2O)_n$ ($n = 20$) cations in the other arrangements for both vertical and adiabatic calculations on the terminal oxygen atom are W1D (0.675, 0.696), W2D (0.741, 0.815), and W3D (0.604, 0.608), respectively. In the case of anionic radicals, the terminal oxygen atom has significantly

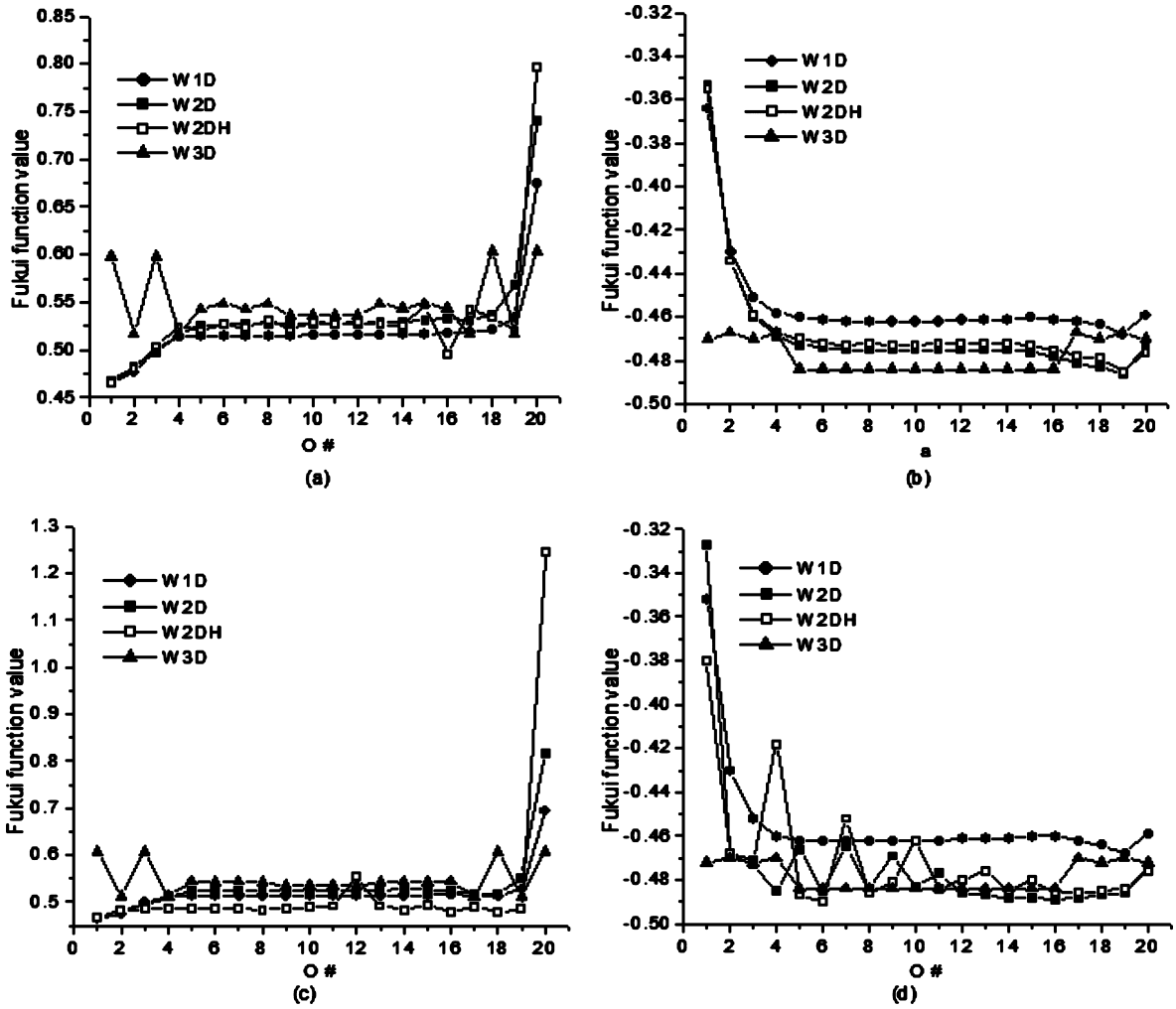

Figure 8. Comparison of Fukui function indices on all oxygen atoms of water eicosamer for four modes of arrangement: (a) IP_V, (b) EA_V, (c) IP_A, and (d) EA_A.

lower Fukui function value compared to rest of the oxygen atoms in the chain. Here, W1D (−0.459, −0.459), W2D (−0.474, −0.474), W2DH (−0.476, −0.476), and W3D (−0.470, −0.472) have aforementioned values in vertical and adiabatic states, respectively. The graphs depicted in Figure 8 plotted on the basis of Fukui function indices against individual oxygen atom help to establish one end of the linear chain as a donor end and the other as acceptor end.

Conclusions

The present paper demonstrates the extent of cooperativity observed in four water cluster arrangements (W1D, W2D, W2DH, and W3D) as a function of chain length. Cooperativity is much more evident as cluster size increases from 2 to 10 rather than from 10 to 20. The caged water clusters seen in W3D arrangement are more stable than the other three linear arrangements at HF, B3LYP, and MP2 levels of theory. The average electron density values (ρ) obtained at the bond critical points using AIM analysis follow the trend W3D > W2DH > W2D > W1D and exhibit a high correlation with complexation energy of all the arrangements. PCM-based implicit solvation yields lower complexation energy in the solvated clusters than the corresponding gas-phase geometries. In all the four arrangements, W2DH clusters show the highest propensity to form cation and anion radicals. Thus, the neutral and ionized water clusters adopt preferentially caged and helical arrangements, respectively.

Acknowledgment. Financial assistance from DAE-BRNS and DST (Swarnajayanthi fellowship to G.N.S., INSPIRE fellowship to Y.I.N., and Women Scientist Fellowship to A.S.M.) is acknowledged. This paper is dedicated to Professor S. R. Gadre on the occasion of his 60th birthday, for his significant contributions to theoretical and computational chemistry over the last three decades.

Supporting Information Available: Geometrical parameters of W1D, W2D, W2DH, and W3D neutral and ionized clusters at B3LYP/6-311+G*, total energies, IP, EA, and Fukui function indices in vertical and adiabatic states of all four arrangements. This material is available free of charge via the Internet at http://pubs.acs.org.

References and Notes

(1) Buckingham, A. D.; Del Bene, J. E.; McDowell, S. A. C. *Chem. Phys. Lett.* **2008**, *463*, 1.

(2) (a) Ludwig, R. *Angew. Chem., Int. Ed.* **2001**, *40*, 1808. (b) Ludwig, R. *ChemPhysChem.* **2000**, *1*, 53.

(3) (a) Suhai, S. *J. Chem. Phys.* **1994**, *101*, 9766. (b) Xantheas, S. S. *Chem. Phys.* **2000**, *258*, 225.

(4) (a) Dannenberg, J. J. *J. Mol. Struct.* **2002**, *615*, 219. (b) Chesnut, D. B. *J. Phys. Chem. A* **2002**, *106*, 6876.

(5) Robert, W.; Laury, H.; Dannenberg, J. J. *J. Phys. Chem. A* **2004**, *108*, 6713.

(6) (a) Liu, K.; Brown, M. G.; Cruzan, J. D.; Saykally, R. J. *J. Phys. Chem. A* **1997**, *101*, 9011. (b) Feyereisen, M. W.; Feller, D.; Dixon, D. A. *J. Phys. Chem.* **1996**, *100*, 2993. (c) Philippe, A.; Christophe, B.; Anthoine,

J.; Delano, P. C. *J. Phys. Chem. A* **2001**, *105*, 7364. (d) Lee, H. M.; Suh, S. B.; Lee, J. Y.; P.; Kim, K. S. *J. Chem. Phys.* **2000**, *112*, 9759.

(7) (a) Tapas, K.; Steve, S. *J. Phys. Chem. A* **2004**, *108*, 9161. (b) Glendening, E. D. *J. Phys. Chem. A* **2005**, *109*, 11936.

(8) (a) Santra, B.; Michaelides, A.; Scheffler, M. *J. Chem. Phys.* **2007**, *127*, 184104. (b) Santra, B.; Michaelides, A.; Fuchs, M.; Tkatchenko, A.; Filippi, C.; Scheffler, M. *J. Chem. Phys.* **2008**, *129*, 194111.

(9) (a) Parthasarathi, R.; Subramanian, V.; Sathyamurthy, N. *J. Phys. Chem. A* **2005**, *109*, 843. (b) Kristin, S. A.; Theodore, S. D.; George, C. S.; Karl, N. K. *J. Phys. Chem. A* **2006**, *110*, 3686.

(10) (a) Hanninen, V.; Salmi, T.; Halonen, L. *J. Phys. Chem. A* **2009**, *113*, 7133. (b) Salmi, T.; Kjaergaard, H. G.; Halonen, L. *J. Phys. Chem. A* **2009**, *113*, 9124.

(11) Gina, H.; Nancy, A.; Marcela, C.; Jorge, D.; Albeiro, R. *J. Phys. Chem. A* **2010**, *114*, 7809.

(12) Maheshwary, S.; Nitin, P.; Sathyamurthy, N.; Kulkarni, A. D.; Gadre, S. R. *J. Phys. Chem. A* **2001**, *105*, 10525.

(13) (a) Parthasarathi, R.; Elango, M.; Subramanian, V.; Sathyamurthy, N. *J. Phys. Chem. A* **2009**, *113*, 3744. (b) Elango, M.; Subramanian, V.; Sathyamurthy, N. *J. Chem. Sci.* **2009**, *121*, 839. (c) Parthasarathi, R.; Subramanian, V.; Sathyamurthy, N. *Synth. React. Inorg. Met.-Org. Nano-Met. Chem.* **2008**, *38*, 18.

(14) Lenz, A.; Ojamae, L. *Phys. Chem. Chem. Phys.* **2005**, *7*, 1905.

(15) Tokmachev, A. M.; Tchougreef, A. L.; Dronskowski, R. *ChemPhysChem* **2010**, *11*, 384.

(16) (a) Nagaraju, M.; Sastry, G. N. *J Phys Chem A.* **2009**, *113*, 9533. (b) Anick, D. J. *J. Phys. Chem. A* **2006**, *110*, 5135. (c) Hu, H.; Lu, Z.; Elstner, M.; Hermans, J.; Yang, W. *J Phys Chem A.* **2007**, *111*, 5685. (d) Deb, N.; Mukherjee, A. K. *Chem. Phys. Lett.* **2008**, *462*, 243. (e) Lee, H. M.; Suh, S. B.; Kim, K. S. *J. Chem. Phys.* **2001**, *114*, 10749.

(17) Ludwig, R.; Appelhagen, A. *Angew. Chem., Int. Ed.* **2005**, *44*, 811.

(18) Wang, L.; Zhao, J.; Fang, H. *J. Phys. Chem. C* **2008**, *112*, 11779.

(19) Hernández-Rojas, J.; Breto'n, J.; Gomez Llorente, J. M.; Wales, D. J. *J. Phys. Chem. B* **2006**, *110*, 13357.

(20) (a) Ghosh, S. K.; Bharadwaj, P. K. *Inorg. Chem.* **2004**, *43*, 6887. (b) Ghosh, S. K.; Bharadwaj, P. K. *Inorg. Chem.* **2004**, *43*, 5180. (c) Ghosh, S. K.; Bharadwaj, P. K. *Angew. Chem., Int. Ed.* **2004**, *43*, 3577.

(21) (a) Long, L.; Wu, Y.; Huang, R.; Zheng, L. *Inorg. Chem.* **2004**, *43*, 3798. (b) Ye, B.; Ding, B.; Weng, Y.; Chen, X. *Inorg. Chem.* **2004**, *43*, 6866. (c) Wang, S.; Xing, H.; Li, Y.; Bai, J.; Pan, Y.; Scheer, M.; You, X. *Eur. J. Inorg. Chem.* **2006**, *45*, 3041. (d) Wang, Y.; Tang, G.; Liu, Z.; Yi, X. *Cryst. Growth Des.* **2007**, *7*, 2272. (e) Zhang, S.; Lan, J.; Mao, Z.; Xie, R.; You, J. *Cryst. Growth Des.* **2008**, *8*, 3134.

(22) (a) Yoshizawa, M.; Kusukawa, T.; Kawano, M.; Ohhara, T.; Tanaka, I.; Kurihara, K.; Niimura, N.; Fujita, M. *J. Am. Chem. Soc.* **2005**, *127*, 2798. (b) Zuhayra, M.; Kampen, W. U.; Henze, E.; Soti, Z.; Zsolnai, L.; Huttner, G.; Oberdorfer, F. *J. Am. Chem. Soc.* **2006**, *128*, 424. (c) Febles, M.; Pérez-Hernández, N.; Pérez, C.; Rodríguez, M. L.; Foces-Foces, C.; Roux, M. V.; Morales, E. Q.; Buntkowsky, G.; Limbach, H.; Martín, J. D. *J. Am. Chem. Soc.* **2006**, *128*, 10008. (d) Miyagawa, T.; Yamamoto, M.; Muraki, R.; Onouchi, H.; Yashima, E. *J. Am. Chem. Soc.* **2007**, *129*, 3676.

(23) (a) Infantes, L.; Motherwell, S. *Cryst. Eng. Commun.* **2002**, *75*, 454. (b) Mir, M. H.; Vittal, J. J. *Angew. Chem., Int. Ed.* **2007**, *46*, 5925. (c) Bergougnant, R. D.; Robin, A. Y.; Fromm, K. M. *Cryst. Growth Des.* **2005**, *5*, 1691. (d) Choudhury, S. R.; Jana, A. D.; Colacio, E.; Lee, H. M.; Mostafa, G.; Mukhopadhyay, S. *Cryst. Growth Des.* **2007**, *7*, 212. (e) Sansam, B. C. R.; Anderson, K. M.; Steed, J. W. *Cryst. Growth Des.* **2007**, *7*, 2649. (f) Saeed, M. A.; Wong, B. M.; Fronczek, F. R.; Venkatraman, R.; Hossain, Md. A. *Cryst. Growth Des.* **2010**, *10*, 1486.

(24) Buch, V.; Sandler, P.; Sadlej, J. *J. Phys. Chem. B* **1998**, *102*, 8641.

(25) Materer, N.; Starke, U.; Barbieri, A.; Van Hove, M. A.; Somorjai, G. A.; Kroes, G. J.; Minot, C. *J. Phys. Chem.* **1995**, *99*, 6267.

(26) Barbour, L. J.; Orr, G. W.; Atwood, J. L. *Nature* **1998**, *393*, 671.

(27) Saha, B. K.; Nangia, A. *Chem. Commun.* **2005**, *3024*.

(28) Nandi, N.; Bagchi, B. *J. Phys. Chem. B* **1997**, *101*, 10954.

(29) Pal, S. K.; Peon, J.; Zewail, A. H. *Proc. Natl. Acad. Sci.* **2002**, *99*, 15297.

(30) Karthikeyan, S.; Kim, K. S. *J. Phys. Chem. A* **2009**, *113*, 9237.

(31) Dahlke, E. D.; Orthmeyer, M. A.; Truhlar, D. G. *J. Phys. Chem. B* **2008**, *112*, 2372.

(32) (a) Williams, C. F.; Herbert, J. M. *J. Phys. Chem. A* **2008**, *112*, 6171. (b) Madarász, A.; Rossky, P. J.; Turi, L. *J. Phys. Chem. A* **2010**, *114*, 2331. (c) Donald, W. A.; Demireva, M.; Leib, R. D.; Aiken, M. J.; Williams, E. R. *J. Am. Chem. Soc.* **2010**, *132*, 4633.

(33) (a) Wales, D. J. *J. Chem. Phys.* **1999**, *110*, 10403. (b) Wales, D. J. *J. Chem. Phys.* **1999**, *111*, 8429. (c) Karthikeyan, S.; Park, M.; Shin, I.; Kim, K. S. *J. Phys. Chem. A* **2008**, *112*, 10120. (d) Park, M.; Shin, I.; Singh, N. J.; Kim, K. S. *J. Phys. Chem. A* **2007**, *111*, 10692. (e) Shin, I.; Park, M.; Min, S. K.; Lee, E. C.; Suh, S. B.; Kim, K. S. *J. Chem. Phys.* **2006**, *125*, 234305. (f) Karthikeyan, S.; Singh, N. J.; Kim, K. S. *J. Phys. Chem. A* **2008**, *112*, 6527.

(34) Lee, H. M.; Suh, S. B.; Tarakeshwar, P.; Kim, K. S. *J. Chem. Phys.* **2005**, *122*, 044309.

(35) (a) Singh, N. J.; Park, M.; Min, S. K.; Suh, S. B.; Kim, K. S. *Angew. Chem., Int. Ed.* **2006**, *45*, 3795. (b) Iyengar, S. S.; Petersen, M. K.; Day, T. J. F.; Burnham, C. J.; Teige, V. E.; Voth, G. A. *J. Chem. Phys.* **2005**, *123*, 084309.

(36) (a) Parthasarathi, R.; Subramanian, V.; Sathyamurthy, N. *J. Phys. Chem. A* **2007**, *111*, 13287. (b) Duan, C.; Wei, M.; Guo, D.; He, C.; Meng, Q. *J. Am. Chem. Soc.* **2010**, *132*, 3321.

(37) (a) Liu, K.; Brown, M. G.; Cruzan, J. D.; Saykally, R. J. *J. Phys. Chem. A* **1997**, *101*, 9011. (b) Paul, J. B.; Provencal, R. A.; Chapo, C.; Roth, K.; Casaes, R.; Saykally, R. J. *J. Phys. Chem. A* **1999**, *103*, 2972. (c) Goldman, B. N.; Leforestier, C.; Saykally, R. J. *Philos. Trans. R. Soc. A* **2005**, *363*, 493.

(38) Douberly, G. E.; Walters, R. S.; Cui, J.; Jordan, K. D.; Duncan, M. A. *J. Phys. Chem. A* **2010**, *114*, 4570.

(39) (a) Egorov, A. V.; Brodskaya, E. N.; Laaksonen, A. *Mol. Phys.* **2002**, *100*, 941. (b) Mata, R. A.; Stoll, H. *Chem. Phys. Lett.* **2008**, *465*, 136.

(40) (a) Hernández-Rojas, J.; González, B. S.; James, T.; Wales, D. J. *J. Chem. Phys.* **2006**, *125*, 224302. (b) James, T.; Wales, D. J.; Hernández-Rojas, J. *J. Chem. Phys.* **2007**, *126*, 054506.

(41) (a) James, T.; Wales, D. J. *J. Chem. Phys.* **2005**, *122*, 134306. (b) Kuo, J. L.; Klein, M. L. *J. Chem. Phys.* **2005**, *122*, 024516. (c) Hodges, M. P.; Wales, D. J. *Chem. Phys. Lett.* **2000**, *324*, 279.

(42) Frank, H. S.; Wen, W. Y. *Discuss. Faraday Soc.* **1957**, *24*, 133.

(43) (a) Reddy, A. S.; Vijay, D.; Sastry, G. M.; Sastry, G. N. *J. Phys. Chem. B* **2006**, *110*, 2479. (b) Reddy, A. S.; Vijay, D.; Sastry, G. M.; Sastry, G. N. *J. Phys. Chem. B* **2006**, *110*, 10206. (c) Vijay, D.; Zipse, H.; Sastry, G. N. *J. Phys. Chem. B* **2008**, *112*, 8863. (d) Vijay, D.; Sastry, G. N. *Chem. Phys. Lett.* **2010**, *485*, 235.

(44) Nagaraju, M.; Sastry, G. N. *Int. J. Quant. Chem.* **2009**, *110*, 1994.

(45) (a) Reddy, A. S.; Zipse, H.; Sastry, G. N. *J. Phys. Chem. B* **2007**, *111*, 11546. (b) Rao, J. S.; Dinadayalane, T. C.; Leszczynski, J.; Sastry, G. N. *J. Phys. Chem. A* **2008**, *112*, 12944. (c) Lee, H. M.; Tarakeshwar, P.; Park, J.; Kołaski, M. R.; Yoon, Y. J.; Yi, H. B.; Kim, W. Y.; Kim, K. S. *J. Phys. Chem. A* **2004**, *108*, 2949.

(46) Rao, J. S.; Zipse, H.; Sastry, G. N. *J. Phys. Chem. B* **2009**, *113*, 7225.

(47) Wales, D. J.; Doye, J. P. K.; Dullweber, A.; Naumkin, F. Y. The Cambridge Cluster Database, http://brian.ch.cam.ac.uk/CCD.html, 1997.

(48) Vijay, D.; Sastry, G. N. *Phys. Chem. Chem. Phys.* **2008**, *10*, 582.

(49) Mahadevi, A. S.; Rahalkar, A.; Gadre, S. R.; Sastry, G. N. *J. Chem. Phys.* **2010**, *133*, 164308.

(50) Frisch, M. J.; Trucks, G. W.; Schlegel, H. B.; Scuseria, G. E.; Robb, M. A.; Cheeseman, J. R.; Montgomery, J. A., Jr.; Vreven, T.; Kudin, K. N.; Burant, J. C.; Millam, J. M.; Iyengar, S. S.; Tomasi, J.; Barone, V.; Mennucci, B.; Cossi, M.; Scalmani, G.; Rega, N.; Petersson, G. A.; Nakatsuji, H.; Hada, M.; Ehara, M.; Toyota, K.; Fukuda, R.; Hasegawa, J.; Ishida, M.; Nakajima, T.; Honda, Y.; Kitao, O.; Nakai, H.; Klene, M.; Li, X.; Knox, J. E.; Hratchian, H. P.; Cross, J. B.; Adamo, C.; Jaramillo, J.; Gomperts, R.; Stratmann, R. E.; Yazyev, O.; Austin, A. J.; Cammi, R.; Pomelli, C.; Ochterski, J. W.; Ayala, P. Y.; Morokuma, K.; Voth, G. A.; Salvador, P.; Dannenberg, J. J.; Zakrzewski, V. G.; Dapprich, S.; Daniels, A. D.; Strain, M. C.; Farkas, O.; Malick, D. K.; Rabuck, A. D.; Raghavachari, K.; Foresman, J. B.; Ortiz, J. V.; Cui, Q.; Baboul, A. G.; Clifford, S.; Cioslowski, J.; Stefanov, B. B.; Liu, G.; Liashenko, A.; Piskorz, P.; Komaromi, I.; Martin, R. L.; Fox, D. J.; Keith, T.; Al-Laham, M. A.; Peng, C. Y.; Nanayakkara, A.; Challacombe, M.; Gill, P. M. W.; Johnson, B.; Chen, W.; Wong, M. W.; Gonzalez, C.; Pople, J. A. *Gaussian 03, Revision C.1*; Gaussian, Inc.: Pittsburgh, PA, 2003.

(51) Boys, S. F.; Bernardi, R. *Mol. Phys.* **1979**, *19*, 553.

(52) (a) Bader, R. F. W. *Atoms in Molecules. A Quantum Theory*; Clarendon: Oxford, UK, 1990. (b) Popelier, P. L. A. *Atoms in Molecules: An Introduction*; Prentice Hall: New York, 2000.

(53) (a) Miertus, S.; Scrocco, E.; Tomasi, J. *J. Chem. Phys.* **1981**, *55*, 117. (b) Tomasi, J.; Persico, M. *Chem. Rev.* **1994**, *94*, 2027.

(54) Li, P.; Bu, Y.; Ai, H. *J. Phys. Chem. A* **2004**, *108*, 1200.

(55) Reed, A. E.; Curtiss, L. A.; Weinhold, F. *Chem. Rev.* **1988**, *88*, 899.

(56) Fukui, K. *Science* **1982**, *218*, 747.

(57) (a) Benco, L.; Tunega, D.; Hafner, J.; Lischka, H. *J. Phys. Chem. B* **2001**, *105*, 10812. (b) Kar, T.; Scheiner, S. *J. Phys. Chem. A* **2004**, *108*, 9161.

JP108634Z